Pulsatile Flow in Microfluidic Systems

Brian Dincau, Emilie Dressaire, Alban Sauret

Department of Mechanical Engineering, University of California, Santa Barbara, CA 93106, USA
E-mail: bdincau@ucsb.edu, dressaire@ucsb.edu, asauret@ucsb.edu

Keywords: ((microfluidics, pulsatile, oscillatory, biomimicry, automation))

This review describes the current knowledge and applications of pulsatile flow in microfluidic systems. Elements of fluid dynamics at low Reynolds number are first described in the context of pulsatile flow. Then the practical applications in microfluidic processes are presented: the methods to generate a pulsatile flow, the generation of emulsion droplets through harmonic flow rate perturbation, the applications in mixing and particle separation and the benefits of pulsatile flow for clog mitigation. The second part of the review is devoted to pulsatile flow in biological applications. Pulsatile flows can be used for mimicking physiological systems, to alter or enhance cell cultures, and for bioassay automation. Pulsatile flows offer unique advantages over a steady flow, especially in microfluidic systems, but also require some new physical insights and more rigorous investigation to fully benefit future applications.

1. Introduction

The precise manipulation of fluids at the submillimeter scale through microfluidics benefits a wide range of applications including material science, microscale physics, *in vitro* diagnostics, drug discovery, biotech process control, and ecological screening.[1–5] This potential was first realized in the development of inkjet printheads, which utilized microfabricated arrays of 10-100 μm nozzles to efficiently and rapidly deliver ink droplets.[6] Their precise control, rapid actuation, and ease of automation allowed microfluidic inkjets to revolutionize the printing industry. However, it has only been over the last two decades that microfluidics has seen tremendous growth in other applications, as microfabrication technologies have become cheaper and more accessible.[1] This has opened many exciting

directions for innovation and new research, giving rise to a dynamic field of microfluidics-based research.

Over this period, sophisticated microfluidic devices have emerged, demonstrating rapid cell sorting,[7] ultrasensitive analyte detection,[8,9] monodisperse microdroplet emulsification, [10] precise micro pumping ,[11–13] and biosample purification.[14,15] These have utilized a variety of different transport phenomena which can be broadly categorized as either capillary, pressure-driven, centrifugal, electrokinetic, and acoustic transport.[1] Regardless of the transport scheme, microfluidic devices are all characterized by submillimeter length scales, giving rise to physical relationships which differ considerably from macroscale flows. Herein lie numerous advantages which have enabled so many novel microfluidic applications, as well as some clear limitations which have made it challenging for these new applications to reach the scalability and ubiquity of inkjet printing. Many of these limitations are tied to the nature of steady laminar flow in microchannels.[16] Recent reports suggest that these limitations may be overcome using more complex unsteady flows.

Laminar flows through circular and rectangular channels can be solved analytically, while flows in more complicated geometries can be solved with high accuracy using simulation software.[17] This allows for microfluidic designs to be prototyped and fine-tuned using digital models before investing in any microfabrication. While this simplicity is desirable from a design standpoint, several challenges come with laminar transport, one of which is reagent mixing.

For a reagent or chemical species with mass diffusivity D, the ratio of advective to diffusive mixing is described by the Péclet number (*Pé*). At the macroscale, mixing is generally dominated by turbulent transport. But in low Reynolds number (*Re*) flows, the mixing speed is controlled by the diffusivity of reagents. In a rectangular microchannel, this can result in mixing lengths larger than 1000 times the channel width.

Several inertial microfluidic strategies have emerged in the last decade, which use higher flow velocities to reach $Re \sim 100$ to leverage inertial effects in fluid mixing and particle transport.[18,19] Another technique is to increase the channel length to ensure sufficient reagent mixing before the next microfluidic operation. However, both strategies (increasing channel length or flow velocity) incur a significant energy cost, as the necessary pressure difference scales with both channel length and velocity for incompressible flow through constant cross-section microchannels. These pressures often necessitate rigid fabrication materials such as glass and silicon [20] and pose a significant challenge for point-of-care or consumer applications

due to the cost of fabrication and limited access to external high-pressure sources.[21] Another option is to depart from steady unidirectional flow and take advantage of fluid oscillations.[22]

Pulsatile flow is an unsteady flow in which any arbitrary flow property can be decomposed into a time-averaged and oscillatory component. Oscillatory flows are a specific category of pulsatile flows, having only an oscillatory component with zero time-averaged components. In the mixing problem outlined above, it is possible to take advantage of the viscous nature of these low-*Re* flows, which require negligible energy to accelerate or decelerate. Instead of using the channel geometry to increase its length, using an oscillatory velocity to periodically switch the flow direction increases the effective travel distance without requiring an increased pressure.[23] This increase in effective length is just one example of how pulsatile flow has been used in microfluidics, with numerous other examples in recent literature, many of which are far more complex. The time variance of pressure, velocity, shear stress, etc. in pulsatile flows has been used for enhanced separation and mixing,[24] microdroplet pinch-off and control,[25] efficient on-chip process automation,[23,26] and clog mitigation.[27,28]

In addition to their added complexity for enhanced microfluidic functions, pulsatile flows also possess significant biological relevance. Nearly all macroscopic animals rely on some sort of open or closed circulatory system, through which fluid transport is driven by a pulsatile heartbeat. Indeed, many cardiovascular flows are modeled as pulsatile flows through chambers or channels.[29] Even organisms which possess no heart or complex circulatory systems, such as jellyfish, sponges or fungi, often rely on unsteady flows in their environment to circulate nutrients and waste.[30] The pulsatile environment plays a critical role in the growth, motion, and development of many cell types.[31–33] As a result, many biologists have begun to incorporate pulsatile flows in their experiments. However, the characterization of pulsatile flow in these studies is often incomplete, due to a lack of standardization for describing and controlling parameters of the pulsatile flow. As more and more studies emerge, consistent nomenclature and control strategies will be paramount in establishing the cross-disciplinary knowledge needed to fully utilize pulsatile microsystems.

This review provides a brief primer outlining some important physical phenomena in pulsatile flows, and what these mean in the context of microfluidics. It then presents a summary of the state-of-the-art in microfluidic systems which utilize pulsatile flows to reach new levels of functionality across a broad range of applications. Finally, this review addresses the importance of pulsatile flows in biological systems, in particular, to enhance cell culture efficacy and mimic physiological conditions in biomicrofluidic experiments.

2. Physical Description of Pulsatile and Oscillatory Flows

The majority of microfluidic systems have relied on steady flows in rigid or deformable devices. To enable new functionalities, a few studies have focused on how to leverage pulsatile flows. While steady flows are time-invariant, pulsatile flows present a new time scale associated with the oscillation of the flow. These systems are commonly driven by an external oscillating harmonic field. For example, a microfluidic flow driven by a pulsatile pressure difference Δp can be written as

$$\Delta p = \Delta p_0 + \delta p \, e^{i\omega t}$$

where Δp_0 is the time-averaged pressure, δp denotes the amplitude of the pressure oscillation, and ω is the frequency of the oscillation.

With this expression, several different flow fields can be defined, as shown in **Figure 1**. When the oscillation amplitude is zero ($\boldsymbol{\delta p = 0}$), time variance disappears, leaving classical steady flow (**Figure 1**a). When $\boldsymbol{\delta p \neq 0}$**,** two types of harmonic flow can be defined. Pulsatile flow describes the case when $\boldsymbol{\Delta p_0 \neq 0}$, as shown in **Figure 1**b. In this situation, there is an average advection of fluid particles with an oscillatory amplitude of $\boldsymbol{\delta p}$ and angular frequency $\boldsymbol{f = \omega/(2\pi)}$ superposed on it. Oscillatory flow describes the case when $\boldsymbol{\Delta p_0 = 0}$, hence fluid particles experience no net advection over time, but rather oscillate about a central position.

To characterize the influence of flow oscillations for varying microfluidic chip designs, it is also necessary to take into account the characteristics of the system. The Reynolds number (Re) describes the magnitude of inertial forces relative to viscous forces in a flow, described by $Re = UL/\nu$, where U and L are the characteristic velocity and length scales respectively,

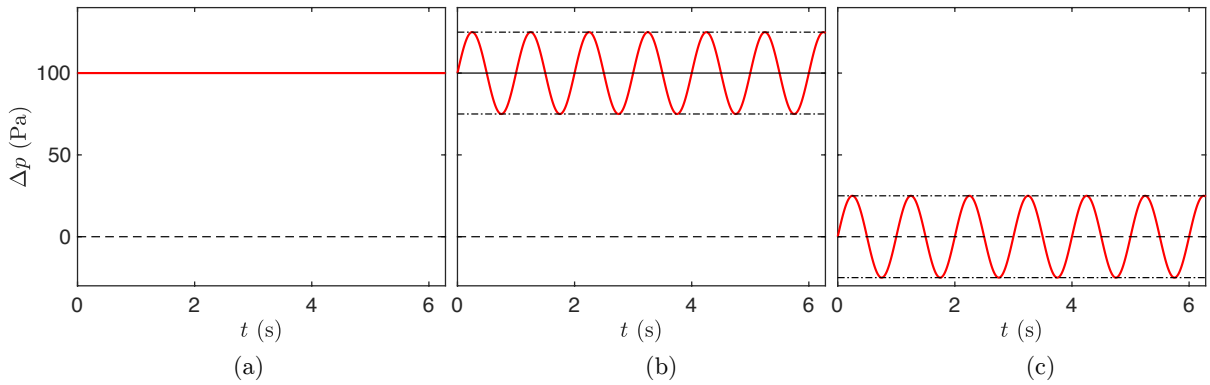

Figure 1 - Characteristic steady and transient flow schemes. For each plot, time is represented on the independent axis, and the dependent axis represents a flow-related variable such as velocity, pressure, or shear rate. (a) Steady flow has a non-zero mean value and no oscillatory component. (b) Pulsatile flow has non-zero mean value, with periodic time-varying oscillations about that mean. (c) Oscillatory flow has zero or near-zero mean value, with periodic time-varying oscillations about that mean.

while ν is the kinematic viscosity of the fluid, defined as the ratio of dynamic viscosity η to density ρ such that $\nu = \eta/\rho$. A typical microfluidic device (utilizing water as the working fluid $\nu \approx 10^{-6}\, m^2 s^{-1}$, average velocity $U \in [10^{-6}, 10^{-2}]\ ms^{-1}$, and channel width $L \in [10^{-6}, 10^{-4}]\ m$) possesses a range of $10^{-6} < Re < 1$.[16] Therefore, viscous effects tend to dominate fluid transport in microfluidic systems, yielding laminar flows. However, *Re* does not contain any parameters to account for the time-varying aspects of pulsatile and oscillatory flows.

In a pulsatile environment, the fluid flow can be subjected to both viscous resistance and inertia resulting from the pulsatile nature of the system, even at low *Re*. This situation is different from steady flow in microchannels, where only viscous resistance is relevant. As a result, an additional dimensionless parameter needs to be introduced. The Womersley number (Wo) compares the transient inertial effects to viscous forces, [34] defined as:

$$Wo = \left(\frac{\omega\, L^2}{\nu}\right)^{1/2}$$

For $Wo \ll 1$, viscous effects dominate, and the oscillation frequency of the flow is sufficiently small, such that the steady velocity profile has time to develop during each cycle. For instance, in a cylindrical capillary, the steady-state Poiseuille profile is recovered at each oscillation cycle for low *Wo*. The opposite situation, where the oscillation frequency is sufficiently large, leads to $Wo \gg 1$ and corresponds to the situation in which the oscillatory inertial force dominates the dynamics and strongly modifies the mean flow profile. In this regime, when the pressure gradient is reversed, it takes some time before the pressure gradient can change the direction of the flow, which leads to a phase shift between the fluid flow and the pressure gradient. For instance, in blood vessels, the Womersley number typically ranges from $Wo \sim 15$ for the larger vessels (aorta, large veins) to $Wo \sim 10^{-3}$ for the smaller capillaries.[34] Thus the flow profile for larger vessels is significantly modified and out of phase with the pressure field, while the flow profile for smaller vessels is in phase with the pressure field.

Another important aspect that neither *Re* nor *Wo* capture is the relative amplitude of oscillation $\xi = \delta p/\Delta p_0$. ξ also captures the approximate flow state where $\xi \ll 1$ corresponds to steady flow, $\xi \gg 1$ corresponds to oscillatory flow and $\xi \sim 1$ corresponds to pulsatile flow. While this parameter is not commonly used in contemporary pulsatile studies, it completes the non-dimensional description of pulsatile flow. *Re* describes the laminarity of the flow, *Wo* describes the flow response to oscillatory forcing, and ξ describes the flow as steady, pulsatile, or oscillatory. For studies that seek to produce physiologically relevant pulsatile flows in microsystems, matching the values for *Re*, *Wo*, and ξ is thus crucial.

The analytical resolution of single-phase flow in the laminar regime can be performed in the case of a rigid microfluidic chip and has been considered, for example, to describe physiological flows. Nevertheless, the influence of flexible microfluidic channels on pulsatile flows is still an active research area that we will mostly neglect in this review, as the effects of compliance and harmonics are highly system-specific.[35–37]

3. Pulsatile Flows in Microfluidic Processes

3.1. Pulsatile Signal Generation

To drive an oscillatory or pulsatile flow in microchannels, external and internal sources can be used to generate an oscillatory signal. External inputs, such as peristaltic pumps or digitally modulated pressure controllers, are perhaps the most straightforward mechanisms for generating a pulsatile signal. Similarly, custom pneumatic channels to superpose oscillatory pressure signals over a steady flow have been used to generate complex pulsatile flows, as illustrated in **Figure 2**.[38,39] While simple and relatively robust, external sources require additional power and space, making them unsuitable of point-of-care or field applications. They are also limited to signal frequencies less than about 15 Hz. As a result, numerous on-chip techniques have been explored.

Generally, on-chip mechanical generation of oscillatory signals is still in early development. Asymmetric elastomeric components have been integrated into microfluidic channels to generate pulsatile flow with constant flow inputs.[40] This technique, analogous to

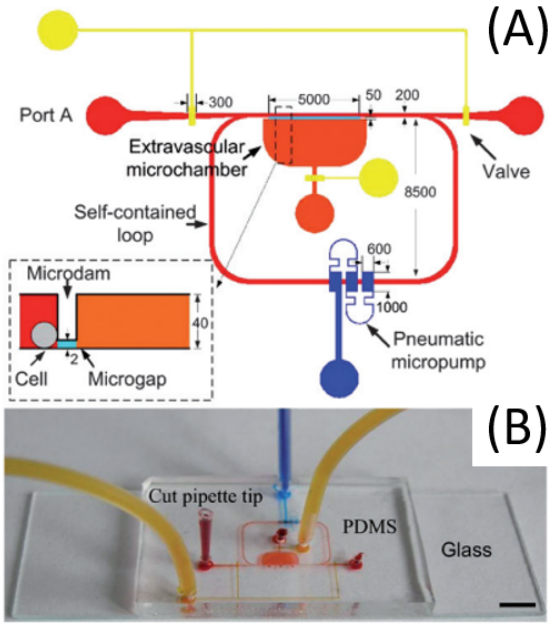

Figure 2 - Pneumatically driven microcirculatory system. (A) Illustration of the circulatory loop (in red), pneumatic micropump (in blue), and valves and extravascular area (in yellow). The exploded view shows a micro gap for cell trapping. Notably, the pneumatic micropump was used to generate a pulsatile flow to recapitulate the physiological shear stress environment of endothelial cells. (B) Photograph of the microcirculatory chip with dye to indicate sections outlined in the schematic, with 5 mm scale bar. Reproduced with permission.[29] Copyright 2009 Royal Society of Chemistry.

an electronic switching circuit, requires that the device be designed as a whole to achieve the desired signal, and has only been demonstrated to reach frequencies as high as 1 Hz. While microfluidic applications are dominated by incompressible flows, microfluidic oscillators made of SU-8 on silicon have been shown to reach near-kilohertz frequencies with compressible flows.[41]

On-chip pulsatile flows are commonly achieved using an oscillatory electrical signal. With origins in inkjet printing, thermal bubble micropumping uses an integrated micro-heater to drive the expansion of an attached bubble. This has been used to impose an oscillatory flow with frequencies up to 300 Hz [42] and can be performed using either Joule [43] or induction [44] heating to influence bubble expansion. Piezoelectric diaphragms have also bee used to induce fluid motion over a wide frequency range.[45–47]

Electrodynamic phenomena can also drive pulsatile flows. In electrowetting, the surface energy between a fluid and dielectric-coated electrode can be manipulated using an applied potential. This is well-suited to microfluidic applications where surface tension alone can be used to drive capillary flows. Electrowetting systems are relatively simple to fabricate, requiring a single-level patterned electrode for basic functionality.[48] Electrowetting can be used to control fluid motion over the patterned electrodes with actuation frequencies in the kilohertz range,[49] with significant potential to enhance micro-scale mixing when combined with droplet-based systems.[50,51]

Electroosmosis is an electrokinetic phenomenon, in which an electric field is used to drive the bulk flow through capillaries or microchannels. Electroosmotic flow (EOF) has the advantage of straightforward, full-channel implementation, similar to electrowetting techniques. However, its sensitivity to electrochemical properties and Joule heating can limit its

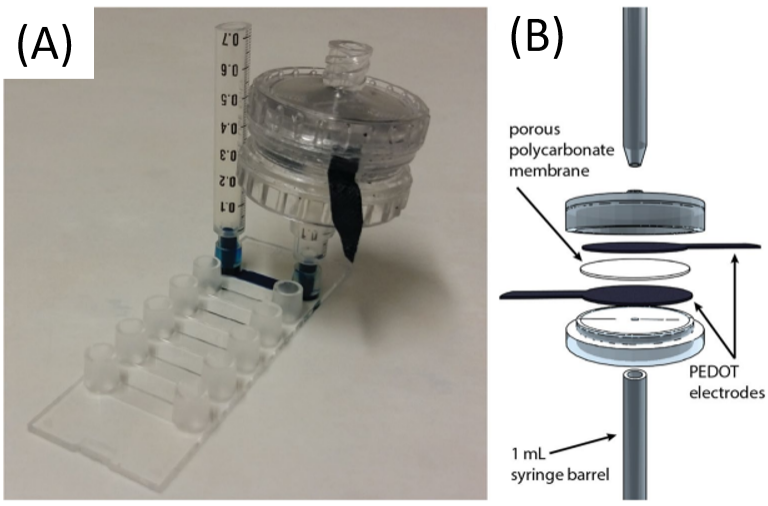

Figure 3 - Modular clip-on electroosmotic pump for oscillating flow. (A) Photograph of the pump and modified syringe filter holder attached to a simple microfluidic culture array filled with blue dye. The pump attaches with a standard Luer connector. (B) Exploded schematic of the modified syringe filter holder and pump, consisting of a porous polycarbonate membrane and two poly(3,4-ethylene dioxythiophene) polystyrene sulfonate (PEDOT:PSS) electrodes. Reproduced with permission.[57] Copyright 2018 springer.

applicability to a variety of samples.[52] Oscillatory EOF is still in early development, with numerous theoretical studies emerging.[53–56] Bengtsson *et al.* recently developed a clip-on electroosmotic pump with standardized Luer connectors for microfluidic cell culture devices, shown in **Figure 3**. This device could easily be adapted for other oscillatory microfluidic flows.[57] It has the advantages of low-cost, low-footprint, and easy implementation with demonstrated oscillatory flow rates of $\pm$400 μL min^{-1} and frequencies up to 0.25 Hz.

This summary illustrates the wide variety of techniques that can be used to generate oscillatory signals, which include a mix of active, passive, external, and on-chip strategies. On one hand, this variety is advantageous for designing microfluidic systems which may operate over a wide range of flow rates or handle samples with a variety of thermal, electrical, and viscous properties. On the other hand, this variety presents a challenge in describing the effects of pulsatile flows across such a wide range of operating conditions. For instance, many of the strategies reported above focus primarily on oscillatory frequency, while only a few specifically mention mean flow rate and oscillatory amplitude. Eventually, a more complete description of pulsatile parameters will be required to compare different techniques and standardize pulsatile studies across disciplines critically.

3.2. Droplet Generation

One classical application of microfluidic technologies is droplet generation and control, which has become a versatile tool with applications in material synthesis,[58–60] high-throughput biochemical screening,[61,62] and single-cell analysis.[63–66] Droplet-based systems possess the advantages of low reagent use, scalable production of droplets, a high-surface-area-to-volume ratio which facilitates fast reactions, and independent droplet control.[67] Most applications demand high uniformity in droplet size, but some applications require well-controlled sequences of droplets with different volumes.[25] Managing droplet coalescence is also critical in systems which use microdroplets for encapsulation of miniature reaction volumes.[68] In any case, precise control of droplet size, formation, and motion are essential.

Early systems have utilized passive droplet generation techniques, in which constant flow rates or pressures are enforced in a two-phase microfluidic junction. The flow is driven by syringe pumps or pressure controllers, and the energy of the system is partially converted into interfacial energy which destabilizes the liquid-liquid interface and can induce droplet formation or corrugations of the jet.[10,69,70] Passive techniques for droplet generation rely on the spontaneous growth of Rayleigh-Plateau instabilities to trigger droplet formation.[71] While channel geometry can be used to passively induce or suppress droplet breakup,[72] pressure and

flow rate are the only tunable parameters. Electric fields can also be used to influence droplet breakup of dielectric jets,[73] but requires suitable working fluids. This means passive techniques are limited in droplet size, generation frequency, and appropriate fluid choice.[70,74] Instead, active techniques have emerged to provide additional flexibility in droplet size and production rate while also improving the system response time needed for stable droplet production.[25,75]

Pulsatile flow is essential to numerous active droplet generation techniques. The pulsatile condition provides additional control over droplet formation, as it removes the dependence on Rayleigh-Plateau instability growth. Triggering the droplet formation with external forcing is particularly useful in generating droplets having very low interfacial tension. Such is the case for aqueous two-phase systems (ATPS).[76,77] While passiIn this case, a constant continuous-phase input and pulsatile disperse-phase input have been used to generate monodisperse ATPS droplets ranging from 10 pL to 10 nL.[78–82] Notably, the pulsatile frequency (0 to 200 Hz) and amplitude (1 to 3 mm) impact the synchronization of glycerol-in-oil droplets generation.[83] Indeed, pinch-off dynamics induced by these pressure fluctuations are highly dependent on the initial perturbations.[84]

Droplet formation can also be induced by vibrations. Using a traditional passive capillary injection coupled with an active loudspeaker and membrane, ATPS droplet generation frequencies as high as 1 kHz have been demonstrated,[85] which is roughly 100 times faster than the natural frequency for droplet formation for this system. Finally, pulsatile flows also provide

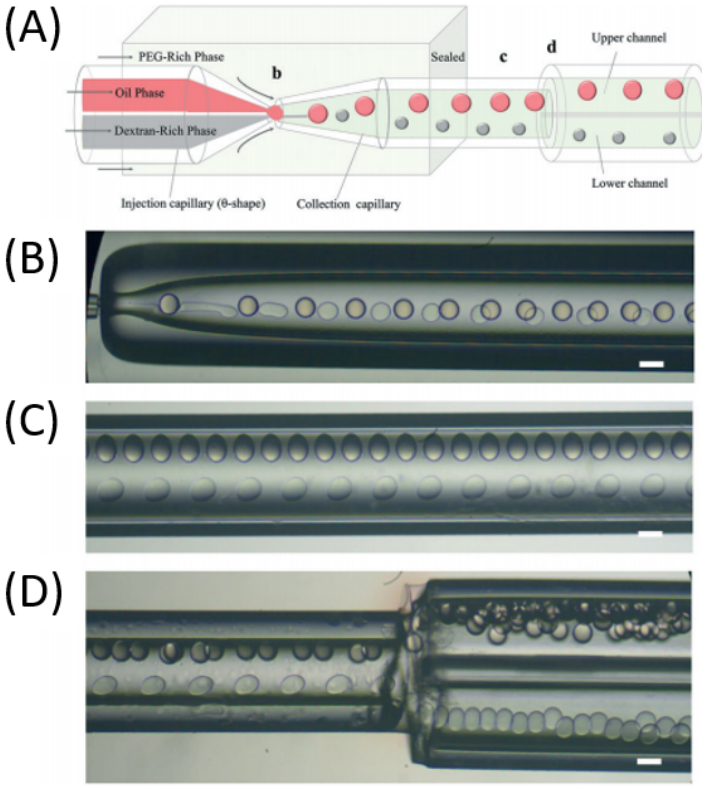

Figure 4 - Oil-chopper based microdroplet generator. (A) Illustrative schematic of device operation with the oil-phase shown in red and aqueous phase in grey. (B) Pulsatile inputs to the oil-phase create oil microdroplets which perturb the adjacent continuous aqueous phase. This triggers rapid instability growth and aqueous droplet formation. (C) Oil and aqueous droplets are separated by density and then (D) collected in a theta-shaped capillary. Scale bars are 200 µm. Reproduced with permission. [87] Copyright 2017 Royal Society of Chemistry.

additional control over the position and shape of the individual droplet in confined flows.[86] These aspects are not only directly useful in the design of droplet-based microfluidic systems, but may also shed light on the dynamical features of physiological systems, such as red blood cells in pulsatile flows.

A unique strategy introduced by Zhou *et al.* combines the benefits of both passive and active methods. This method involves perturbations induced by secondary oil droplets, termed "choppers," to distort an adjacent aqueous surface and induce droplet formation in the aqueous phase.[87] While both the oil and aqueous phases are introduced via steady flow, the passive breakup of the high-surface tension oil jet triggers oscillatory perturbations in the aqueous jet, which leads to spontaneous active droplet formation. This was demonstrated at frequencies up to 2.1 kHz for droplet sizes ranging from 20 μm to 300 μm, having a coefficient of variance between 0.75% and 2.45% for droplet diameter. Oil and ATPS droplets were then separated by density in a θ-shaped glass capillary. The droplet generation, separation, and collection steps of this method are depicted in **Figure 4**.

3.3. Enhanced Mixing

Mixing is often a crucial step in functional microfluidics, especially in material synthesis and bioassays. [24,88,89] Traditional microfluidic devices operate in a low-*Re* regime, yielding laminar flow profiles in which mixing is limited by diffusion. To improve upon this, more complex geometries in steady flow regimes can induce two-dimensional stretching and folding of fluid elements, which increases the interfacial area between segregated fluids to facilitate faster mixing. This process is termed chaotic mixing.[88] In addition to geometric elements, such as herringbone or serpentine channels, hydrodynamic focusing is also used to fold segregated fluids and enhance mixing times repeatedly.[89] Pulsatile strategies can also significantly improve mixing times, especially if coupled with other enhancements.

The simplest pulsatile mixing strategy is to add an oscillatory component to an otherwise-steady mixing interface. An early demonstration of this combined two aqueous fluids at a y-connection and used a pinch valve on each arm to generate strong pulsations, while a peristaltic pump provided the mean flow.[90] With this setup, Truesdell *et al.* performed a set of experiments to investigate the relative effects of pulse period, pulse width, and delay. They note that in cases of improved mixing, the mixing interface appears fractal, while the interface remains undisturbed under poor mixing conditions.

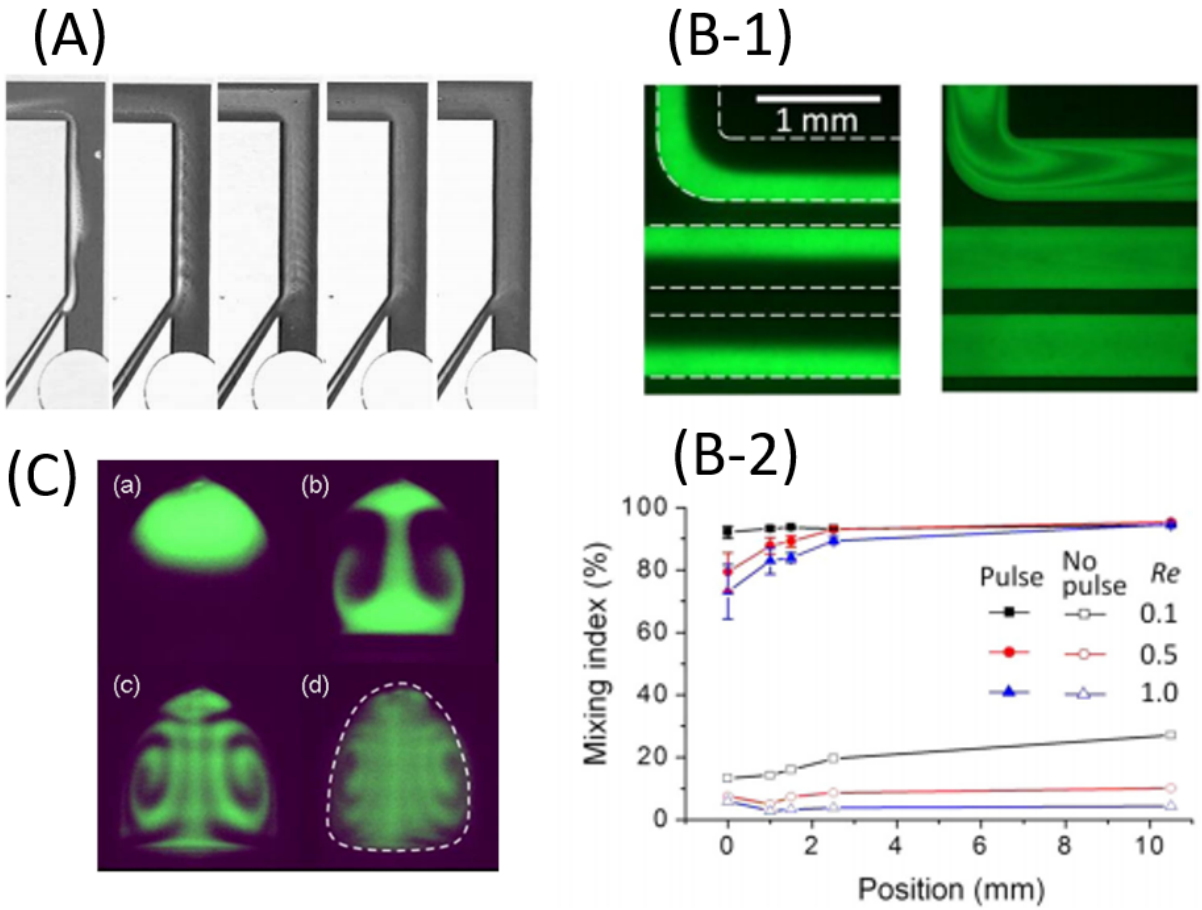

Figure 5 - Examples of mixing enhancement by oscillatory perturbations. (A) Mixing of IPA and blue dye in a microchannel improve with increasing oscillatory frequency. From left to right: 5, 50, 100, 150, and 200 Hz. Reproduced with permission. [43] Copyright 2001 Elsevier. (B-1) Comparison of streamwise mixing in straight and elbow microchannels under steady flow (left) and 18 Hz pulsatile flow (right). (B-2) Plot comparing the mixing index in the streamwise direction, demonstrating significantly faster mixing under pulsatile conditions. Reproduced with permission. [91] Copyright 2016 Elsevier. (C) Time-lapse of mixing in a droplet due to electrowetting-induced oscillatory motion at 81 Hz, with approximately 0.55 seconds between images. Reproduced with permission. [51] Copyright 2006 AIP Publishing.

Another early demonstration was performed by Tsai *et al.*, who used a thermal bubble micropump to generate an oscillatory flow in a microfluidic mixer.[43] They found that mixing of blue food dye and isopropyl alcohol improved with increasing oscillatory actuation frequency, with optimal mixing achieved around 200 Hz, as depicted in **Figure 5**a.

Recently, Li *et al.* presented a microfluidic device which does not rely on any off-chip dynamic controllers to achieve pulsatile mixing.[91] They used integrated valves and elastomeric membranes to generate an oscillatory signal. The authors report a five- to twenty-fold improvement in mixing index at a switching frequency of 18 Hz when compared to a steady, diffusion-limited case as summarized in **Figure 5**b.

Depending on the sample type and additional required functionalities, several other strategies to enhance mixing with a pulsatile flow have been proposed. For example, pulsatile

flows can be combined with geometry to induce rotational flows via circular mixing chambers,[92] or amplify chaotic mixing through converging-diverging nozzles[93] or cross-flow junctions[94]. Another promising technique leverages the internal convection of a confined moving droplet to enhance mixing.

A confined droplet or fluid plug, which is in interfacial contact with the surrounding microchannel, will experience internal circulation as it moves through the channel. Stone *et al.* developed a model which predicts enhanced mixing in a spherical droplet subject to external flows,[95] while enhanced mixing in confined droplets has been experimentally demonstrated and visualized.[96,97] Mugele *et al.* added oscillatory motion to the droplet via transient electrowetting to further improve mixing speed, while also decreasing the required channel length.[51] They used an oscillatory frequency between 10 and 125 Hz to enhance mixing time by two orders of magnitude over pure diffusion in millimeter-sized droplets. The time evolution of one droplet, initially labeled heterogeneously with a fluorescent dye, is shown in **Figure 5**c.

Mixing is a major microfluidic operation which has seen drastic improvements when enhanced by pulsatile flows. Whether through simple flow reversal to increase mixing time without increasing device footprint, high-frequency fluid oscillations to induce chaotic mixing, or internal circulation using droplet techniques, pulsatile strategies can improve mixing times by an order of magnitude over steady flow counterparts. Nevertheless, determining the optimal oscillatory parameters has largely been an empirical process, thus there remains significant room for the development of new models to describe pulsatile mixing environments.

The applications of pulsatile flows to multiphase systems goes beyond the mixing of two liquids. The motion of particles in suspension can be altered by the addition of a time-dependent component of the flow field.

3.4. Particle Separation and Control

Particle manipulation is an enabling function for many microfluidics systems. Inert microparticles, such as those made of polystyrene, are frequently used to demonstrate particle operations including separation, concentration, and focusing.[98] Functional micro- and nanoparticles, such as magnetic or bio-conjugated beads, allow for more sophisticated particle manipulation via external fields or specific adsorption of target molecules to enhance bioassays.[99] Droplets, cells, bacteria, viruses, and even large macromolecules such as DNA[100] are all particles ranging in size from tens of nanometers to hundreds of micrometers.[101] Due to the variety of particle sizes and physical properties, manipulation cannot be achieved using the

same technique for all applications, inspiring a surge in the development of passive and active particle manipulation platforms over the last two decades.[102,103]

While the majority of microfluidic operations involving particles have been performed with a steady flow, pulsatile and oscillatory environments have enabled novel functionality. One challenging aspect of low-*Re* inertia-less flows is their reversibility, which must be overcome in pulsatile systems. This has been done by designing microfluidic features which break the symmetry of the flow, allowing for different particle motion in the forward and reverse directions.

McFaul *et al.* demonstrated a microfluidic funnel ratchet to separate cells based on size and deformability, as illustrated in **Figure 6**.[104] In this device, cells pass through a network of asymmetric tapered constrictions under oscillatory flow conditions generated by a commercial pressure controller. Smaller cells can pass through the constrictions in the forward direction, while larger cells are excluded. Under reverse flow, the smaller cells remain trapped upstream, resulting in repeatable and irreversible cell sorting. The authors report a throughput of approximately 9000 cells per hour with 98% efficiency. They separated peripheral blood mononuclear cells (PBMCs) and mouse lymphoma cells (MLCs) with a sorting area of 3.2 mm x 1.34 mm.

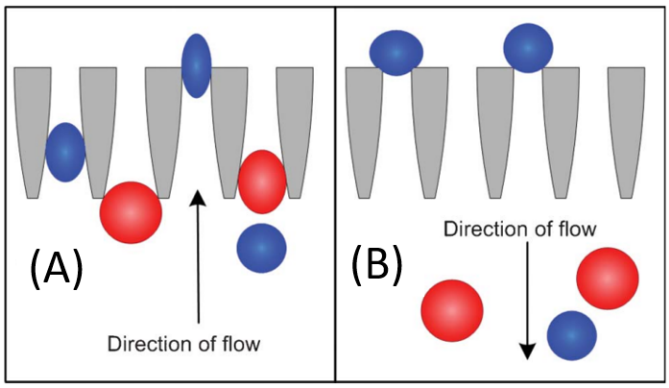

Figure 6 - Illustration describing the operation of a microfluidic oscillatory ratchet for cell sorting. (A) Under forward flow, smaller deformable particles (blue) can pass through the tapered constrictions since they are small enough to fit through the opening. Larger particles (red) cannot squeeze through. (B) Under reverse flow, smaller particles are trapped, as they no longer fit through the reverse openings, while large particles flow in the reverse direction. Organizing these obstructions in an array allows particles to be separated by size under oscillatory flow. Reproduced with permission. [104] Copyright 2012 Royal Society of Chemistry.

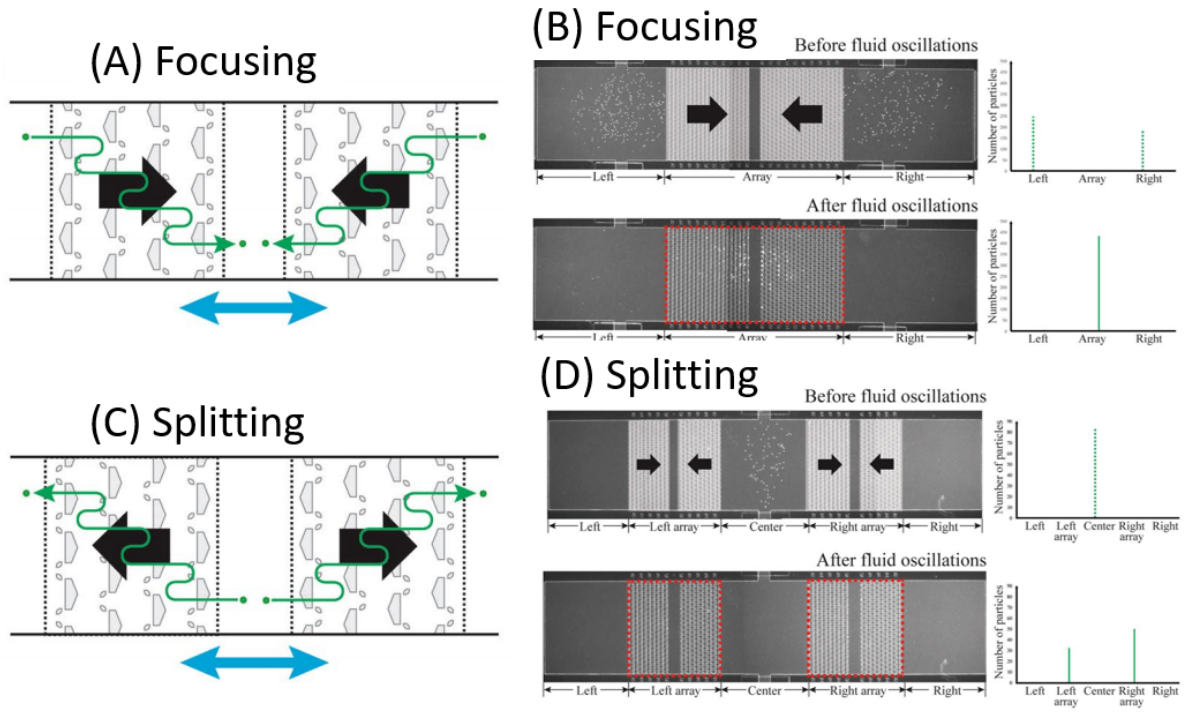

Figure 7 - Particle operations performed in an asymmetric obstacle array under oscillatory flow. (A) Illustration showing particle focusing under oscillatory flow when arrays are pointed towards the center. (B) Micrographs taken before and after particle focusing, with corresponding histograms to quantify particle migration. (C) Illustration showing particle splitting under oscillatory flow when arrays are pointed away from the center with (D) corresponding micrographs and histograms. Reproduced with permission. [110] Copyright 2019 Springer Nature.

A similar technique was used by Cheng *et al.* to perform single cell capture, array, release, and labeling with a relatively simple design.[26] They used a two-dimensional trap array to filter 2 μm beads from 12 μm beads with 92.7% efficiency under a 1 Hz pulsatile flow, however separation of circulating tumor cells (CTCs) from whole blood was challenging due to the significant overlap in sizes of CTCs and white blood cells (WBCs). Based on similar works, CTC isolation could be improved by deformability-based separation,[105–109] rather than size-based separation, while still benefitting from the reduced footprint and simplicity of operations facilitated by the pulsatile flow strategy.

Recently, Lee *et al.* demonstrated a passive microfluidic chip capable of both particle sorting and focusing using a similar combination of asymmetric obstacles and oscillatory flow.[110] They use an array of asymmetric traps, depicted in **Figure 7**, to uniquely influence particle migration in both the forward and reverse direction. They demonstrate size-based segregation with > 95% efficiency, solution exchange (i.e., washing), and focusing/splitting of particle suspensions on a closed fluidic circuit requiring minimal external equipment.

Oscillatory flows have also been implemented in inertial microfluidics, which perform particle focusing and manipulation in microchannels using inertial lift forces.[18] One limitation

to inertial microfluidics is the strong correlation between particle size and the inertial lift force. Particles smaller than a few microns require prohibitively long channel lengths to reach their focusing position, on the order of a few meters. However, an oscillatory flow strategy enables microchannels to have an infinite effective length, enabling the inertial focusing of small particles in relatively short channels. This was demonstrated by Mutlu *et al.* in 2017, who used a 10 to 20 Hz oscillatory flow to focus a variety of particles as small as 500 nm in 10 seconds.[111] In addition to focusing, other modes of self-assembly are possible in oscillatory inertial microfluidic systems.[112]

In all of these strategies, a major advantage of oscillatory flows is the reduction in device footprint, since flow switching increases the effective channel length without increasing the actual physical length. The particle operations are therefore performed over an infinite effective length without incurring significant losses due to drag forces, which leads to unique operations when the forward and reverse flows are asymmetric. Additionally, many of the works reviewed above demonstrate superior reliability and claim that oscillatory systems exhibit a lower susceptibility to clogging than equivalent steady-flow techniques. This is extremely promising for high-throughput particle operations such as blood fractionation or rare-cell isolation, which are often limited by their operational robustness.

3.5. Clog Mitigation

A considerable obstacle to the commercialization and widespread use of microfluidics is their propensity for clogging. Whether due to accidental contamination with impurities or an accumulation of target particles themselves, clogging is typically detrimental to microfluidic systems, which can be prohibitively difficult to clean or reset once the flow is impeded.[113] Until this issue is adequately addressed, microfluidic platforms may continue to suffer from a low adoption rate. As a result, there has been a push to understand the complex problem of clogging at the single-pore[114,115] and even single-particle level,[116] to better predict and model the growth of clogs.[117] All of these fundamental clogging studies have focused on steady flow, but recent reports have found that clogging can be effectively mitigated with the aid of oscillatory perturbations.

Under steady inertia-less flow, particles which become clogged are most likely to remain clogged. However, periodic oscillations can re-orient particles to delay or eliminate the onset of clogs. For example, in the previously mentioned study by McFaul *et al.*, the oscillatory flow was not only essential in controlling particle motion in the microfluidic chip, but also played a significant role in clog mitigation. The authors operate the system continuously for

more than four hours without any degradation in functionality.[104] An oscillatory flow strategy was also used to mitigate clogging in the previously mentioned microdevice by Cheng *et al.*, using a 1Hz pressure fluctuation as their oscillatory condition.[26]

In 2016, Cheng *et al.* demonstrated a clogging-free platform for cell separation from undiluted blood, which is highly susceptible to clogging.[118] They used a bidirectional micropump to enable reverse flushing of micropores to prevent clogging of the commercially available polycarbonate membranes. Their bidirectional flow strategy highlights the impact of oscillatory motion in clog prevention. At the same time, Yoon *et al.* used a piezoelectric actuator to add 130 Hz fluid oscillations to a micro-sieving system capable of size-based separation of polystyrene particles and cancer cells with 100% separation efficiently and 98% retrieval.[28] They used the same device to separate cancer cells from whole blood, during which fluid oscillations prevent the micro-sieve from becoming clogged by filtered cancer cells, allowing continuous separation with high efficiency. Partially-clogged, flowing, and filtered samples are shown in **Figure 8**.

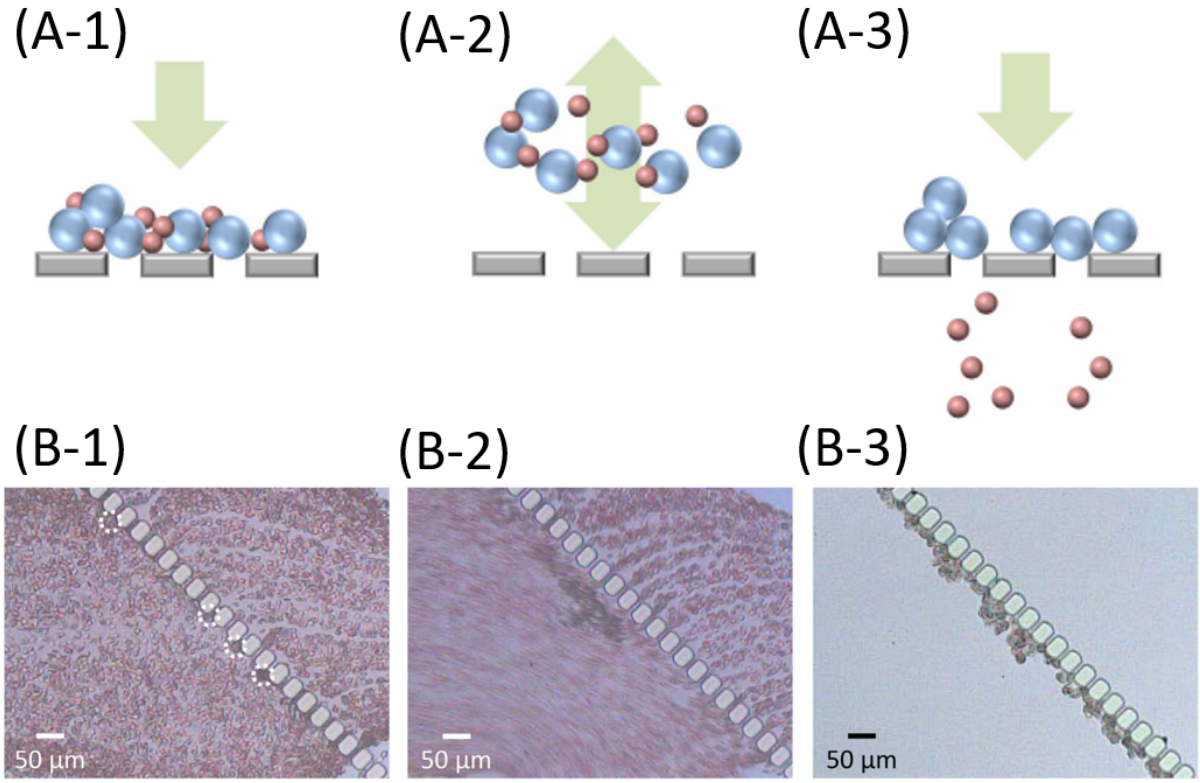

Figure 8 - Clog mitigation via oscillatory flow. (A) Illustration demonstrating the impact of oscillatory flow in clog mitigation. (A-1) Small and large particles become packed against the filter, resulting in a clog. (A-2) Oscillatory flow continuously clears the filter space to prevent clog formation. (A-3) Small particles continue to flow through the filter, allowing large particles to be enriched. (B) Micrographs of a continuous µ-sieve device for the enrichment of cancer cells in whole blood. (B-1) A filter region which is partially clogged by a combination of cells. White dotted circles indicate the cancer cells. (B-2) Clog-free sieving under oscillatory flow. (B-3) Enriched cancer cells after sieving the spiked blood sample. Reproduced with permission.[28] Copyright 2016 Springer Nature.

Another whole blood device, developed by Mehendale *et al.*, uses a radial array of pillars and a vibration motor to achieve clogging-free operation.[27] The radial flow pattern results in dynamic cross-flow regions as certain pathways become more constricted, while the attached vibration motor helps to disturb cell clusters which would otherwise clog the array. The oscillatory frequency of the vibration motor was not explicitly discussed.

Across these studies, we note that the oscillation frequency can vary significantly while still mitigating clog formation. Some authors have reported frequencies as low as 1Hz, and as high as 200 Hz, while some authors do not report their oscillatory parameters. Based on the works reviewed, pulsatile flows provide some benefit to clog mitigation, but there is still much to learn in terms of optimization and physical mechanisms. The dynamics of clogging and clog mitigation in microfluidic systems is still a growing topic, and a rigorous study of clogging in pulsatile systems has yet to be conducted.

Despite the current gaps in pulsatile flow mechanisms and parameter standardization, numerous groups have already used pulsatile flows for droplet generation, enhanced mixing, particle control, and clog mitigation. These signals can be generated in a variety of ways, each with their own strengths and limitations, giving rise to a wide range of platforms. Many of these have been utilized in biological studies spanning the molecular- to tissue-level, as pulsatile flows are ubiquitous throughout living systems.[29,30] Additionally, the range of operations enabled by pulsatile flow techniques makes them extremely attractive for the automation of standard bioassays.

4. Applications of Pulsatile Flows in Biology

4.1. Biomimicry for Physiological Studies

Biological experiments are a cornerstone to critical advancements in drug discovery, genetic mapping, and biophysics. [119] Generally, these experiments are challenging because rigorous control is difficult to achieve with living systems, hence repetition and multiplexing are heavily utilized to improve the clarity and significance of results.[120] Furthermore, they may require exotic, expensive reagents which can become prohibitive. To directly address these issues, biological experiments have now utilized microfluidic platforms for decades,[121] allowing for reduced reagent consumption and better environmental controls, such as cell localization and environment sterility. Indeed, numerous groups have taken advantage of lab-on-a-chip platforms to automate multiplex processes and generate results at an accelerated rate.[122]

The underlying assumption of these *in vitro* experiments is that the results offer some insight about *in vivo* biology. To satisfy this assumption, the *in vitro* models seek to mimic relevant aspects of the *in vivo* environment. This includes the mechanical environment of the biological system.[123] For example, endothelial cells, which line the inside of the cardiovascular system (CVS), are exposed to shear forces resulting from blood flow.[29] These forces are driven by the heartbeat and are pulsatile in nature with $Wo > 1$ in many regions of the CVS. Therefore, steady flow is insufficient in recapitulating the stress environment of many endothelial cells, and there has been significant interest in capturing the pulsatile nature of cardiovascular flows.[124,125] Shear stress was experimentally determined in vivo in 1980, using the feline mesentery as a model system spanning a wide range of vasculature levels at a scale similar to that of a human.[126,127] Pulsatile microfluidic environments can hence be tuned to mimic *in vivo* conditions and provide greater physiological relevance.

Using a pulsatile flow chamber, Chien *et al.* compared endothelial cell (EC) gene expression and morphological changes under steady, oscillatory, and pulsatile flow conditions.[128] While the authors used an oscillatory pump to generate various pulsatile flow conditions, it is also possible to convert a steady flow perfusion system into a pulsatile system using a set of switches to periodically redirect flow, as illustrated in **Figure 9**a.[129] Using similar techniques, numerous groups have demonstrated a variety of mechanical feedback mechanisms which yield distinct responses under pulsatile flow conditions.[125,128,130] In 2006, Wang *et al.* showed that expression of Krüppel-like factor 2, which is essential to EC differentiation and

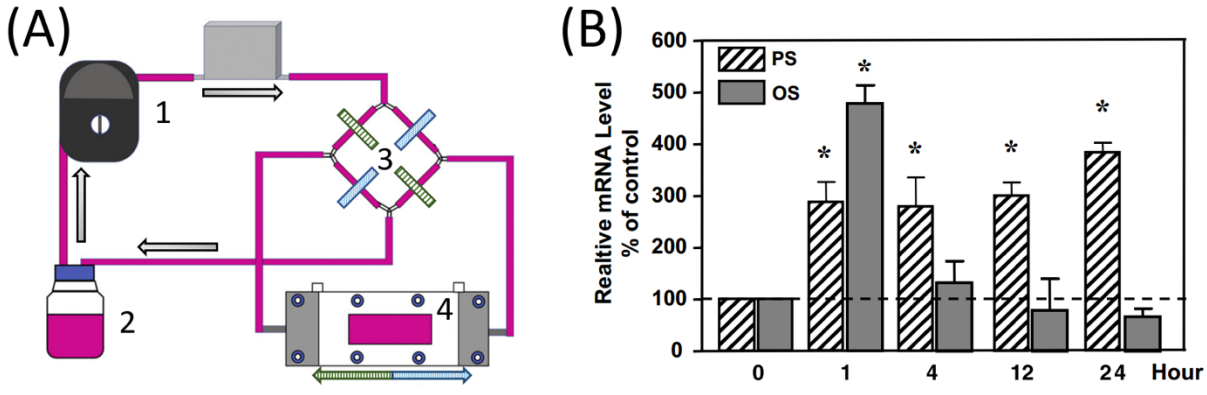

Figure 9 - Oscillatory flow for investigating the effects of physiological shear stress on cultured endothelial cells (ECs). (A) Illustration of an oscillatory parallel plate flow chamber. The pump (1) draws fluid from the reservoir (2) at a constant speed. Directional control switches (3) are used to open and close hoses, generating a pulsatile flow through the perfusion chamber (4). Reproduced with permission.[129] Copyright 2019 Elsevier. (b) Flow-pattern specific regulation of Krüppel-like factor 2 (KLF2) in ECs exposed to either pulsatile flow (PS) or oscillatory flow (OS) compared to the static control. The horizontal dashed line represents KLF2 expression in the static control group, while PS and OS levels are normalized as a percentage of the static control. RNA samples were isolated at 0, 1, 4, 12, and 24 hours after exposure to pulsatile or oscillatory flow and quantified via real-time RT-PCR. Reproduced with permission. [131] Copyright 2006 Elsevier.

development, is different under static, oscillatory, and pulsatile flow condition, reported in **Figure 9**b.[131] Similar experiments have demonstrated that endothelial cells respond to oscillatory shear stress with increased expression of miRNA-663[132] and Toll-like receptor 2 (TLR2),[129] both of which are highly associated with an inflammatory response. Therefore, mimicking the pulsatile nature of cardiovascular flows is essential to understanding inflammatory diseases like atherosclerosis and even aneurysm progression.[133] Numerous cardiovascular organ-on-a-chip (OOC) platforms have emerged over the past decade, and have just recently begun incorporating complex flows to emulate the *in vivo* stress environment.[134]

Physiological pulsatile flows are not limited to the cardiovascular system. Eyes are coated by a thin film of tears, which is subject to an oscillatory flow generated by blinking. Blinking helps to clear debris from the cornea, as well as redistribute tears to maintain hydration.[135] The oscillatory shear forces associated with blinking may also be an essential signal for corneal epithelial cell growth and maintenance. Corneal epithelial cells were grown under static, steady, and oscillatory conditions, then compared using a combination of scanning electron microscopy and immunofluorescence. Cells grown under oscillatory conditions exhibit drastic differences in cell morphology and expression of cell junctions when compared to steady flow and static control.[136] This emphasizes the importance of accurately capturing the transient shear environment when modeling ocular surface pathology, especially when tear film may be compromised, such as with contact lenses and chronic dry eyes.

Oscillatory flows emerge in many other natural settings as well, which may require translation to microfluidic platforms for simplified study. Tidal environments are inherently subject to oscillatory forcing from waves, as well as long-term oscillations in their local environment as the sea waxes and wanes. This has an extreme impact on the spacial heterogeneity in coastal aquifers[137] and the lifecycle and feeding habits of benthic organisms.[138] Many of these marine animals are microscopic and use small hair-like filaments called cilia to sense their environment and capture food particles. These cilia generate micro-pulsatile flows to pump food particles toward them, which has inspired several groups to model synthetic oscillating cilia for microparticle capture[139] and asymmetric oscillatory signal generation.[140] Additionally, many microswimmers rely on asymmetric oscillatory forcing to move through their environment.[141,142] Platforms which can precisely control oscillatory force environments are essential in studying these diverse organisms and interactions. The initial efforts toward the development of such platform have focused on cell culture, in which a single species or community of cells are grown under controlled conditions. When these organisms

are sensitive to shear stress, the nature of their flow environment can affect their growth and proliferation; hence, pulsatile flows have seen increased use in cell culture protocols.

4.2. Enhanced Cell Culturing

Cell culture is a fundamental component of biomedical research, enabling the investigation of cellular and molecular mechanisms, pharmaceutical development, and regenerative medicine.[143] Naturally, there is a demand for miniaturizing the cell-culture environment using microfluidic technologies to reduce media consumption, improve sterility, and provide greater control.[144] In particular, microfluidics enables the precise manipulation of shear forces experienced by cells, with well-characterized and highly repeatable flow profiles. For many cell lines, the shear stress environment significantly affects cell growth and development.[124,125,145] Therefore, oscillatory flows may better mimic physiological flow conditions, giving rise to improved cell proliferation and viability.

It is well-understood that endothelial cells (ECs) possess mechanosensitive feedback mechanisms which are highly sensitive to the shear flow environment.[146] Depending on the mean shear stress and oscillatory shear stress, the feedback mechanisms can bolster or impede endothelial cells growth. Generally, a pulsatile environment with relatively high mean shear stress has demonstrated positive effects on endothelial cells growth, while oscillatory environments are correlated with inflammation and disordered cell morphology.[39] But endothelial cells are not the only cell type to respond to pulsatile culture systems.

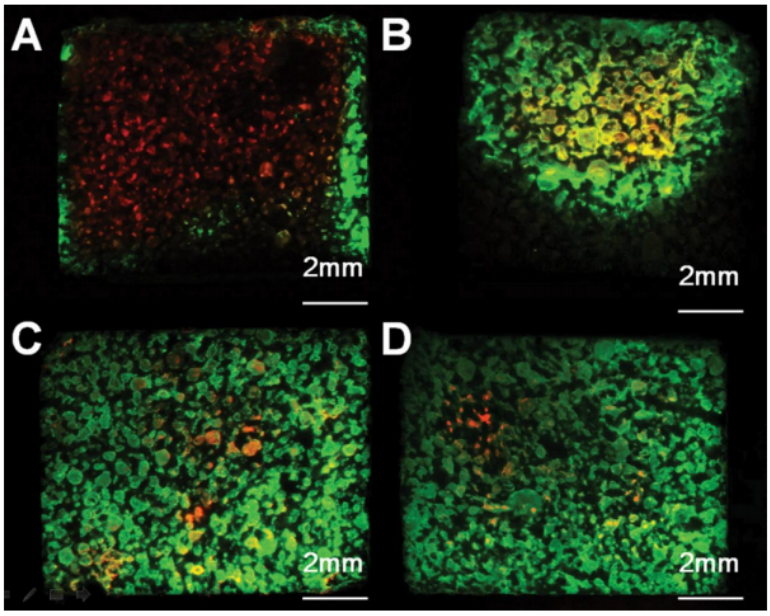

Figure 10 - Effects of oscillatory shear stress on osteoblast-like cells. Cells are stained with Calcein-AM to indicate live cells (green) and propidium iodide to indicate dead cells (red). Each frame represents a different flow condition: (A) static culture, (B) steady perfusion at 1 mL/min, (C) pulsatile perfusion at 0.5 mL/min, (D) pulsatile perfusion at 1 mL/min. Both pulsatile cultures exhibit superior cell proliferation and viability compared to the static and steady flow cultures. Reproduced with permission.[149] Copyright 2009 Wiley and Sons.

Bone tissues are also subject to a periodic mechanical loading, and the fluid shear stress induced on bone cells *in vivo* is dynamic in nature. Bone marrow stromal cells possess the stem-cell-like ability to differentiate into bone, cartilage, adipose, and hematopoietic supporting tissues based on chemical and physical differentiation cues.[147] Oscillatory techniques benefit the culture of these cells for regenerative therapies. Human marrow stromal cells subject to pulsatile flow in parallel plate flow channels exhibit increased proliferation and intracellular Ca^{2+} mobilization.[148] Similarly, mouse osteoblast-like cells exhibit significantly improved viability and proliferation uniformity under pulsatile flow conditions when compared to steady and static flow conditions in 3D culture, as illustrated in **Figure 10**.[149]

4.3. Automation of PCR and Other Bioassays

Polymerase Chain Reaction (PCR) is a nucleic acid amplification technique heavily utilized in biomedical research and forensic investigations.[150] Multiplex PCR enables the amplification of several distinct DNA templates in the same reaction volume, which reduces the total time and effort required.[151] Most conventional PCR systems rely on macroscale thermal cycling, which can take 2 – 3 hours for a 30 – 40 cycle amplification, due to the overall thermal mass and large diffusion lengths. To improve cycle time, microfluidics-based PCR devices have emerged.

Stationary microchamber PCR is a miniaturized analog to conventional PCR. The PCR solution is kept in a stationary well while a micro-heater performs the thermal cycling steps. This system still requires some optimization of thermal mass to minimize reaction times and power consumption.[152] Continuous-flow PCR utilizes pumping to drive the PCR solution through several isolated reaction zones, which improves the temperature transition rate and reaction time. However, continuous flow reactors lack cycle time and cycle number flexibility.[153] Oscillatory flow PCR reactors have been developed to address all of these shortcomings.

Oscillatory PCR reactors also use a moving sample, which can be either single-phase or droplet-based, but modulate the flow speed and direction in an oscillatory manner as illustrated in **Figure 11**. This allows individual reaction zones to be utilized repeatedly, which adds flexibility in accommodating amplification cycles while maintaining a simple, compact platform. These advantages have allowed for simultaneous detection of multiple bacterial pathogens in just 15 minutes, with detection limits comparable to that of conventional PCR.[154–156] Oscillatory flow reverse transcription (RT) PCR reactors, which utilize an additional

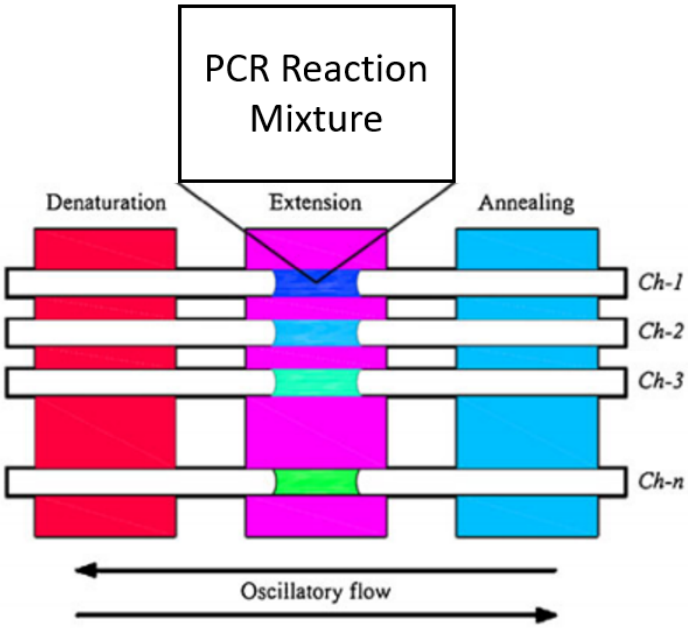

Figure 11 - Illustrative schematic of an oscillatory PCR chamber. PCR mixtures, consisting of primers and DNA templates, are represented by the colored droplets along the center. N channels can be aligned in parallel over the three constant-temperature reaction zones for denaturation, extension, and annealing for multiplex testing. Each channel can be controlled with an independent pressure source, enabling different PCR recipes which correspond to different PCR mixtures. This strategy allows for any number of thermal cycles without increasing the device footprint, while also ensuring reaction homogeneity through mixing induced by oscillatory droplet motion. Reproduced with permission. [155] Copyright 2011 Springer Nature.

enzyme to amplify RNA targets, have also demonstrated similar rapid process times as low as 15 minutes. [157]

With clear advantages in processing speed and footprint reduction, oscillatory flow PCR reactors still have room to grow in complexity and robustness. For example, many of the groups mentioned above have neglected multiplex thermal protocols for PCR, as the annealing temperature for each PCR reaction may be different depending on the template and primer pairs. Nie *et al.* have addressed this by using microheaters and temperature sensors integrated on a silicon substrate and parallel microchannels fabricated in glass or PDMS laminates.[158]

Oscillatory PCR systems will benefit from additional technologies which incorporate sample preparation and real-time detection on-chip. Naturally, these platforms will synergize well with other pulsatile bio-environments used for physiological studies and cell culture, as PCR and RT-PCR are extremely valuable tools for obtaining direct information about gene expression in cells. With growing evidence that highlights the importance of transient stresses in many cells types, combined with all of the functional benefits demonstrated thus far, progress in pulsatile signal generation and pulsatile flow operations will continue to enable physiologically-relevant studies and bioassay automation in microsystems.

5. Conclusions and Perspective

Microfluidic devices have been increasingly used over the last two decades to take advantage of several attributes that come with miniaturization. Ideally, their small footprint and multifunctionality allow for portable use with minimal user experience. Their sub-millimeter

scale often results in low-*Re* flows, which can start and stop almost instantaneously with high repeatability. Micron-scale features allow for precise manipulation of micron- and submicron-scale particles, such as red blood cells, cancer cells, bacteria, viruses, and designer micro- and nanoparticles. But microfluidic devices also suffer from their own set of unique challenges, some of which may be overcome using pulsatile or oscillatory flows. Many studies have emerged which demonstrate oscillatory enhancements in mixing, low interfacial tension droplet generation, particle manipulation, and clog mitigation. Additionally, recent biological studies have focused on the incorporation of pulsatile flows to improve the physiological relevance of in vivo system, enhance cell cultures, and automate bioassays such as PCR. However, a great deal of these studies has also left many open questions to be addressed with future work.

A distinct lack of turbulent transport in low-*Re* flows means that mixing of heat, momentum, and chemical species is limited by their respective diffusivities. Mixing by diffusion can be prohibitively long; thus, tremendous effort has been spent on improving mixing times in microfluidic systems. Recently, we have seen numerous oscillatory techniques which can be easily combined with existing chaotic mixing strategies to significantly enhance mixing time. This is particularly beneficial in the automation and rapidization of bioassays, which often rely on mixing for chemical labeling and thermal cycling.

The dominance of interfacial effects at the microscale has enabled an era of precise droplet generation and control. Aqueous two-phase system (ATPS) droplets are desirable for their extreme biocompatibility, which makes them ideal platforms for cell encapsulation[159] and biomolecule delivery.[160] However, stable generation of ATPS droplets is challenging under steady flow, as Rayleigh-Plateau instability growth is slow with low interfacial tension. The addition of oscillatory perturbations has been demonstrated to remove the dependence on passive instabilities, allowing for ATPS droplet generation at frequencies as high as 2 kHz, spanning a wide range of droplet volumes.

The challenge of clogging has always plagued microfluidic systems, especially when handling complex samples such as whole blood. As a result, many microfluidic functionalities are only demonstrated with highly controlled samples, such as microbeads in water. Eventually, clog formation and clog mitigation must be understood to facilitate the development of robust microfluidic systems, which can be successfully operated without clogging outside of the laboratory environment. Several groups have recently utilized a variety of pulsatile flow strategies to periodically reset particles and delay or prevent the onset of clogging. These strategies vary tremendously in their oscillatory parameters, indicating that almost any significant oscillatory input may reduce clogging susceptibility.

The applications of mixing, droplet generation, particle control, and clog mitigation have made oscillatory microfluidics an ideal platform for cell manipulation and miniaturization of bioassays, such as PCR. Additionally, pulsatile and oscillatory flows themselves are desirable for developing physiologically relevant models in which *in vivo* oscillatory conditions are significant, such as the cyclic stresses experienced in blood flow and bone loading. Indeed, we have seen that adding oscillatory conditions to traditional cell culture systems can alter cell growth and proliferation, demonstrating the importance of oscillatory control when optimizing culture protocols or investigating the impact of oscillatory stresses *in vitro*.

With all of these applications emerging in the last decade or so, pulsatile microfluidics is still in its infancy. The move from steady to pulsatile input conditions increases design complexity in several respects. The addition of oscillatory frequency and amplitude represent two additional control parameters which affect the transient flow profile and overall system functionality. The influence of harmonics, especially in compliant systems such as those made of PDMS or other elastomers, means that these oscillatory parameters are coupled with the system itself. This complicates the design process, as harmonic effects can alter effective impedance and damping force at the microscale must be considered. Measuring, controlling, and reporting these parameters will be essential in the development of broadly-applicable pulsatile theories.

As new applications emerge, developing a more thorough understanding of pulsatile systems will greatly benefit microfluidics as a whole. Microfluidics has recently experienced a push toward modularity[161–163] to improve adoption rate by decreasing the need for custom lithographic devices. This presents an excellent opportunity for designing modular fluid oscillators, which eliminate the dependence on outside equipment to generate the oscillatory signal. However, given the complexity of pulsatile flows in microsystems, fundamental characterization and optimization of oscillatory parameters for the applications mentioned in this review represent an essential step in standardizing the implementation of modular microfluidic oscillators. With that established, simplified inclusion of pulsatile flows in microfluidic systems will contribute to a new era of functionality and reliability, which will greatly benefit existing microfluidic assays and processes, and help enable the widescale development and commercialization of microfluidic solutions.

Table of Contents Entry

Pulsatile Flow in Microfluidic Systems
Brian Dincau, Alban Sauret, Émilie Dressaire**

This review outlines the fundamental parameters describing pulsatile flows and summarizes contemporary applications in microfluidic systems and biological studies. These include pulsatile signal generation, droplet emulsion, accelerated mixing, particle separation, clog mitigation, mimicking *in vivo* pulsatile environments, enhanced cell culturing, and bioassay automation. Their added complexity expands microfluidic functionality, yet many opportunities to refine pulsatile flow theory and implementation remain. **Keyword -** Pulsatile

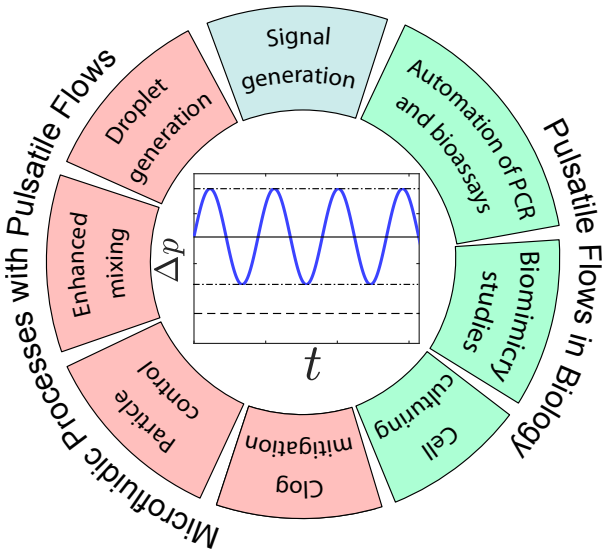

Brian Dincau is a Ph.D. student at the University of California Santa Barbara (UCSB). He received his Master's Degree in Mechanical Engineering in 2018 from Washington State University Vancouver (WSUV), during which he studied biosensors and high-throughput microfluidics. He received his Bachelor's degree in Mechanical Engineering in 2012 from the University of California Davis (UCD) with a minor in Technology Management. He has experience working in the semiconductor and HVAC industries. His research focuses on the intersection of biology, fluid dynamics, and microsystems and how they can be leveraged in a new era of scalable bioprocessing and biomanufacturing.

Emilie Dressaire is an Assistant Professor in the Department of Mechanical Engineering at the University of California Santa Barbara (UCSB). She graduated with a Ph.D. in Mechanical Engineering at Harvard University. Previously, she was a faculty member in the Mechanical and Aerospace Engineering Department at NYU Tandon School of Engineering and a research scientist at CNRS. Her research interests are centered around the areas of small scale fluid mechanics and soft matter physics, specifically focusing on interdisciplinary projects to develop bio-inspired methods to control and monitor fluid flows.

Alban Sauret is an Assistant Professor in the Department of Mechanical Engineering at the University of California Santa Barbara (UCSB). Previously, he studied at ENS Lyon, received his PhD from Aix-Marseille University in France, and was a postdoctoral researcher at Princeton University. Before joining UCSB, he was CNRS Research Scientist. His research aims at understanding the dynamics of multiphase systems. He is particularly interested in the couplings between the fluid dynamics, interfacial effects, and particle transport mechanisms involved in industrial and environmental processes.

References

[1] D. Mark, S. Haeberle, G. Roth, F. von Stetten, R. Zengerle, *Chem. Soc. Rev.* **2010**, *39*, 1153.
[2] N. Yogarajah, S. S. H. Tsai, *Environ. Sci. Water Res. Technol.* **2015**, *1*, 426.
[3] L. KANG, *Drug Discov. Today* **2008**, *13*, 1.
[4] X. Mao, T. J. Huang, *Lab Chip* **2012**, *12*, 1412.
[5] P. S. Dittrich, A. Manz, *Nat. Rev. Drug Discov.* **2006**, *5*, 210.
[6] E. Bassous, H. H. Taub, L. Kuhn, *Appl. Phys. Lett.* **1977**, *31*, 135.
[7] C. W. S. IV, C. D. Reyes, G. P. López, *Lab Chip* **2015**, *15*, 1230.
[8] C. Zhao, Z. Ge, C. Yang, *Micromachines* **2017**, *8*, 28.
[9] G. Luka, A. Ahmadi, H. Najjaran, E. Alocilja, M. DeRosa, K. Wolthers, A. Malki, H. Aziz, A. Althani, M. Hoorfar, *Sensors* **2015**, *15*, 30011.
[10] R. Seemann, M. Brinkmann, T. Pfohl, S. Herminghaus, *Reports Prog. Phys.* **2011**, *75*, 16601.
[11] G. M. Walker, D. J. Beebe, *Lab Chip* **2002**, *2*, 131.
[12] D. J. Laser, J. G. Santiago, *J. Micromechanics Microengineering* **2004**, *14*, R35.
[13] Y.-N. Wang, L.-M. Fu, *Microelectron. Eng.* **2018**, *195*, 121.
[14] R. J. Meagher, Y. K. Light, A. K. Singh, *Lab Chip* **2008**, *8*, 527.
[15] M. Sonker, V. Sahore, A. T. Woolley, *Anal. Chim. Acta* **2017**, *986*, 1.
[16] T. M. Squires, S. R. Quake, *Rev. Mod. Phys.* **2005**, *77*, 977.
[17] J. Wang, V. G. J. Rodgers, P. Brisk, W. H. Grover, *PLoS One* **2017**, *12*, e0189429.
[18] D. Di Carlo, *Lab Chip* **2009**, *9*, 3038.
[19] D. Di Carlo, D. Irimia, R. G. Tompkins, M. Toner, *Proc. Natl. Acad. Sci.* **2007**, *104*, 18892.
[20] J. Cruz, S. H. Zadeh, T. Graells, M. Andersson, J. Malmström, Z. G. Wu, K. Hjort, *J. Micromechanics Microengineering* **2017**, *27*, 84001.
[21] E.-C. Yeh, C.-C. Fu, L. Hu, R. Thakur, J. Feng, L. P. Lee, *Sci. Adv.* **2017**, *3*, e1501645.
[22] G. Cai, L. Xue, H. Zhang, J. Lin, *Micromachines* **2017**, *8*, 274.
[23] M. Abolhasani, K. F. Jensen, *Lab Chip* **2016**, *16*, 2775.
[24] K. Ward, Z. H. Fan, *J. Micromechanics Microengineering* **2015**, *25*, 94001.
[25] P. Zhu, L. Wang, *Lab Chip* **2017**, *17*, 34.
[26] D. Cheng, Y. Yu, C. Han, M. Cao, G. Yang, J. Liu, X. Chen, Z. Peng, *Biomicrofluidics* **2018**, *12*, 34105.
[27] N. Mehendale, O. Sharma, S. Pandey, D. Paul, *Biomed. Microdevices* **2018**, *20*, DOI 10.1007/s10544-018-0319-z.
[28] Y. Yoon, S. Kim, J. Lee, J. Choi, R.-K. Kim, S.-B. S.-J. Lee, O. Sul, S.-B. S.-J. Lee, *Sci. Rep.* **2016**, *6*, DOI 10.1038/srep26531.
[29] C. G. Caro, *The Mechanics of the Circulation*, Cambridge University Press, **2011**.
[30] S. Vogel, *Life in Moving Fluids 2nd Ed.*, Princeton University Press, **1994**.
[31] C. F. Dewey Jr., S. R. Bussolari, M. A. Gimbrone Jr., P. F. Davies, *J. Biomech. Eng.* **1981**, *103*, 177.
[32] C. T. Hung, S. R. Pollack, T. M. Reilly, C. T. Brighton, *Clin. Orthop. Relat. Res.* **1995**, 256.
[33] Y. Liu, J.-H. Tay, *J. Appl. Microbiol.* **2001**, *90*, 337.
[34] J. R. Womersley, *J. Physiol.* **1955**, *127*, 553.
[35] J. R. Womersley, *Phys. Med. Biol.* **1957**, *2*, 178.
[36] C. J. Morris, F. K. Forster, *Exp. Fluids* **2004**, *36*, 928.
[37] F. Sharipov, D. Kalempa, *Microfluid. Nanofluidics* **2007**, *4*, 363.
[38] J. Lee, Z. Estlack, H. Somaweera, X. Wang, C. M. R. Lacerda, J. Kim, *Lab Chip* **2018**, *18*, 2946.

[39] J. Shao, L. Wu, J. Wu, Y. Zheng, H. Zhao, Q. Jin, J. Zhao, *Lab Chip* **2009**, *9*, 3118.
[40] B. Mosadegh, C.-H. Kuo, Y.-C. Tung, Y. Torisawa, T. Bersano-Begey, H. Tavana, S. Takayama, *Nat. Phys.* **2010**, *6*, 433.
[41] E. W. Simões, R. Furlan, R. E. B. Leminski, M. R. Gongora-Rubio, M. T. Pereira, N. I. Morimoto, J. J. S. Avilés, *Flow Meas. Instrum.* **2005**, *16*, 7.
[42] S.-C. Chan, C.-R. Chen, C.-H. Liu, *Sensors Actuators A Phys.* **2010**, *163*, 501.
[43] J.-H. Tsai, L. Lin, *Sensors Actuators A Phys.* **2002**, *97–98*, 665.
[44] B. Liu, J. Sun, D. Li, J. Zhe, K. W. Oh, *Microfluid. Nanofluidics* **2016**, *20*, DOI 10.1007/s10404-016-1822-2.
[45] L.-S. Jang, S.-H. Chao, M. R. Holl, D. R. Meldrum, *Sensors Actuators A Phys.* **2005**, *122*, 141.
[46] J. Xu, D. Attinger, in *Encycl. Microfluid. Nanofluidics*, Springer US, **2013**, pp. 1–10.
[47] B. Zhao, X. Cui, W. Ren, F. Xu, M. Liu, Z.-G. Ye, *Sci. Rep.* **2017**, *7*, DOI 10.1038/s41598-017-10785-1.
[48] J. Kedzierski, S. Berry, B. Abedian, *J. Microelectromechanical Syst.* **2009**, *18*, 845.
[49] F. Mugele, J.-C. Baret, *J. Phys. Condens. Matter* **2005**.
[50] A. Klingner, S. Herminghaus, F. Mugele, *Appl. Phys. Lett.* **2003**, *82*, 4187.
[51] F. Mugele, J.-C. Baret, D. Steinhauser, *Appl. Phys. Lett.* **2006**, *88*, 204106.
[52] B. J. Kirby, *Micro- And Nanoscale Fluid Mechanics*, Cambridge University Press, **2010**.
[53] G. Ramon, Y. Agnon, C. Dosoretz, *Microfluid. Nanofluidics* **2010**, *10*, 97.
[54] J. C. Misra, S. Chandra, G. C. Shit, P. K. Kundu, *Appl. Math. Mech.* **2014**, *35*, 749.
[55] M. Peralta, J. Arcos, F. Méndez, O. Bautista, *Fluid Dyn. Res.* **2017**, *49*, 35514.
[56] I. Medina, M. Toledo, F. Méndez, O. Bautista, *Chem. Eng. Sci.* **2018**, *184*, 259.
[57] K. Bengtsson, J. Christoffersson, C.-F. Mandenius, N. D. Robinson, *Microfluid. Nanofluidics* **2018**, *22*, DOI 10.1007/s10404-018-2046-4.
[58] J. H. Kim, T. Y. Jeon, T. M. Choi, T. S. Shim, S.-H. Kim, S.-M. Yang, *Langmuir* **2013**, *30*, 1473.
[59] T. Kong, J. Wu, M. To, K. Wai Kwok Yeung, H. Cheung Shum, L. Wang, *Biomicrofluidics* **2012**, *6*, 034104.
[60] R. K. Shah, H. C. Shum, A. C. Rowat, D. Lee, J. J. Agresti, A. S. Utada, L.-Y. Chu, J.-W. Kim, A. Fernandez-Nieves, C. J. Martinez, D. A. Weitz, *Mater. Today* **2008**, *11*, 18.
[61] N. Shembekar, C. Chaipan, R. Utharala, C. A. Merten, *Lab Chip* **2016**, *16*, 1314.
[62] T. S. Kaminski, P. Garstecki, *Chem. Soc. Rev.* **2017**, *46*, 6210.
[63] T. P. Lagus, J. F. Edd, *{RSC} Adv.* **2013**, *3*, 20512.
[64] A. M. Klein, L. Mazutis, I. Akartuna, N. Tallapragada, A. Veres, V. Li, L. Peshkin, D. A. Weitz, M. W. Kirschner, *Cell* **2015**, *161*, 1187.
[65] S. Köster, F. E. Angilè, H. Duan, J. J. Agresti, A. Wintner, C. Schmitz, A. C. Rowat, C. A. Merten, D. Pisignano, A. D. Griffiths, D. A. Weitz, *Lab Chip* **2008**, *8*, 1110.
[66] J. Clausell-Tormos, D. Lieber, J.-C. Baret, A. El-Harrak, O. J. Miller, L. Frenz, J. Blouwolff, K. J. Humphry, S. Köster, H. Duan, C. Holtze, D. A. Weitz, A. D. Griffiths, C. A. Merten, *Chem. Biol.* **2008**, *15*, 427.
[67] S.-Y. Teh, R. Lin, L.-H. Hung, A. P. Lee, *Lab Chip* **2008**, *8*, 198.
[68] D. R. Link, E. Grasland-Mongrain, A. Duri, F. Sarrazin, Z. Cheng, G. Cristobal, M. Marquez, D. A. Weitz, *Angew. Chemie Int. Ed.* **2006**, *45*, 2556.
[69] Z. Li, S. Y. Mak, A. Sauret, H. C. Shum, *Lab Chip* **2014**, *14*, 744.
[70] A. Sauret, H. C. Shum, *Int. J. Nonlinear Sci. Numer. Simul.* **2012**, *13*, 351.
[71] A. S. Utada, A. Fernandez-Nieves, H. A. Stone, D. A. Weitz, *Phys. Rev. Lett.* **2007**, *99*, 094502.
[72] Z. Zhang, T. Kong, C. Zhou, L. Wang, *Phys. Rev. Appl.* **2018**, *9*, 024036.

[73] A. Khoshnevis, S. S. H. Tsai, E. Esmaeilzadeh, *Phys. Fluids* **2014**, *26*, 012103.
[74] S. D. Geschiere, I. Ziemecka, V. van Steijn, G. J. M. Koper, J. H. van Esch, M. T. Kreutzer, *Biomicrofluidics* **2012**, *6*, 22007.
[75] J. Li, N. Mittal, S. Y. Mak, Y. Song, H. C. Shum, *J. Micromechanics Microengineering* **2015**, *25*, 84009.
[76] S. Hardt, T. Hahn, *Lab Chip* **2012**, *12*, 434.
[77] Y. Song, A. Sauret, H. Cheung Shum, *Biomicrofluidics* **2013**, *7*, 61301.
[78] B.-U. Moon, S. G. Jones, D. K. Hwang, S. S. H. Tsai, *Lab Chip* **2015**, *15*, 2437.
[79] I. Ziemecka, V. van Steijn, G. J. M. Koper, M. Rosso, A. M. Brizard, J. H. van Esch, M. T. Kreutzer, *Lab Chip* **2011**, *11*, 620.
[80] A. Sauret, H. Cheung Shum, *Appl. Phys. Lett.* **2012**, *100*, 154106.
[81] H. C. Shum, J. Varnell, D. A. Weitz, *Biomicrofluidics* **2012**, *6*, 12808.
[82] P. Zhu, X. Tang, Y. Tian, L. Wang, *Sci. Rep.* **2016**, *6*, 31436.
[83] P. Zhu, X. Tang, L. Wang, *Microfluid. Nanofluidics* **2016**, *20*, DOI 10.1007/s10404-016-1717-2.
[84] P. Zhu, L. Wang, *Chem. Eng. Sci.* **2019**, *196*, 333.
[85] S. Y. Mak, Y. Chao, S. Rahman, H. C. Shum, *Langmuir* **2017**, *34*, 926.
[86] K. Chaudhury, S. Mandal, S. Chakraborty, *Phys. Rev. E* **2016**, *93*, DOI 10.1103/physreve.93.023106.
[87] C. Zhou, P. Zhu, Y. Tian, X. Tang, R. Shi, L. Wang, *Lab Chip* **2017**, *17*, 3310.
[88] J. M. Ottino, S. Wiggins, *Philos. Trans. R. Soc. London. Ser. A Math. Phys. Eng. Sci.* **2004**, *362*, 923.
[89] Y. K. Suh, S. Kang, *Micromachines* **2010**, *1*, 82.
[90] R. A. Truesdell, P. V Vorobieff, L. A. Sklar, A. A. Mammoli, *Phys. Rev. E* **2003**, *67*, DOI 10.1103/physreve.67.066304.
[91] Z. Li, S.-J. Kim, *Chem. Eng. J.* **2017**, *313*, 1364.
[92] J. W. Wu, H. M. Xia, Y. Y. Zhang, P. Zhu, *Mod. Phys. Lett. B* **2018**, *32*, 1840030.
[93] A. Afzal, K.-Y. Kim, *Sensors Actuators B Chem.* **2015**, *211*, 198.
[94] F. R. Phelan, N. R. Hughes, J. A. Pathak, *Phys. Fluids* **2008**, *20*, 23101.
[95] Z. B. Stone, H. A. Stone, *Phys. Fluids* **2005**, *17*, 63103.
[96] H. Kinoshita, S. Kaneda, T. Fujii, M. Oshima, *Lab Chip* **2007**, *7*, 338.
[97] F. Sarrazin, L. Prat, N. Di Miceli, G. Cristobal, D. R. Link, D. A. Weitz, *Chem. Eng. Sci.* **2007**, *62*, 1042.
[98] Y. W. Kim, J. Y. Yoo, *Opt. Lasers Eng.* **2012**, *50*, 87.
[99] B. M. Dincau, Y. Lee, J.-H. Kim, W.-H. Yeo, *Sensors* **2017**, *17*, 2316.
[100] Y.-L. Chen, M. D. Graham, J. J. de Pablo, K. Jo, D. C. Schwartz, *Macromolecules* **2005**, *38*, 6680.
[101] C. Liu, G. Hu, *Micromachines* **2017**, *8*, 73.
[102] P. Sajeesh, A. K. Sen, *Microfluid. Nanofluidics* **2013**, *17*, 1.
[103] A. Lenshof, T. Laurell, *Chem. Soc. Rev.* **2010**, *39*, 1203.
[104] S. M. McFaul, B. K. Lin, H. Ma, *Lab Chip* **2012**, *12*, 2369.
[105] Y. Yoon, J. Lee, M. Ra, H. Gwon, S. Lee, M. Y. Kim, K.-C. Yoo, O. Sul, C. G. Kim, W.-Y. Kim, J.-G. Park, S.-J. Lee, Y. Y. Lee, H. S. Choi, S.-B. Lee, *Cancers (Basel).* **2019**, *11*, 200.
[106] Z. Zhang, J. Xu, B. Hong, X. Chen, *Lab Chip* **2014**, *14*, 2576.
[107] J. S. Kuo, Y. Zhao, P. G. Schiro, L. Ng, D. S. W. Lim, J. P. Shelby, D. T. Chiu, *Lab Chip* **2010**, *10*, 837.
[108] E. S. Park, C. Jin, Q. Guo, R. R. Ang, S. P. Duffy, K. Matthews, A. Azad, H. Abdi, T. Todenhöfer, J. Bazov, K. N. Chi, P. C. Black, H. Ma, *Small* **2016**, *12*, 1909.
[109] S. C. Hur, N. K. Henderson-MacLennan, E. R. B. McCabe, D. Di Carlo, *Lab Chip* **2011**, *11*, 912.

[110] J. Lee, S. E. Mena, M. A. Burns, *Sci. Rep.* **2019**, *9*, DOI 10.1038/s41598-018-37454-1.
[111] B. R. Mutlu, J. F. Edd, M. Toner, *Proc. Natl. Acad. Sci.* **2018**, *115*, 7682.
[112] C. Dietsche, B. R. Mutlu, J. F. Edd, P. Koumoutsakos, M. Toner, *Microfluid. Nanofluidics* **2019**, *23*, DOI 10.1007/s10404-019-2242-x.
[113] E. Dressaire, A. Sauret, *Soft Matter* **2017**, *13*, 37.
[114] H. M. Wyss, D. L. Blair, J. F. Morris, H. A. Stone, D. A. Weitz, *Phys. Rev. E* **2006**, *74*, DOI 10.1103/physreve.74.061402.
[115] A. Marin, H. Lhuissier, M. Rossi, C. J. Kähler, *Phys. Rev. E* **2018**, *97*, DOI 10.1103/physreve.97.021102.
[116] B. Dersoir, A. B. Schofield, M. R. de Saint Vincent, H. Tabuteau, *J. Memb. Sci.* **2019**, *573*, 411.
[117] A. Sauret, K. Somszor, E. Villermaux, E. Dressaire, *Phys. Rev. Fluids* **2018**, *3*, DOI 10.1103/physrevfluids.3.104301.
[118] Y. Cheng, X. Ye, Z. Ma, S. Xie, W. Wang, *Biomicrofluidics* **2016**, *10*, 014118.
[119] E. K. Sackmann, A. L. Fulton, D. J. Beebe, *Nature* **2014**, *507*, 181.
[120] C. Situma, M. Hashimoto, S. A. Soper, *Biomol. Eng.* **2006**, *23*, 213.
[121] F. Su, K. Chakrabarty, R. B. Fair, *IEEE Trans. Comput. Des. Integr. circuits Syst.* **2006**, *25*, 211.
[122] S. K. Hartwell, K. Grudpan, *Microchim. Acta* **2010**, *169*, 201.
[123] C. Hahn, M. A. Schwartz, *Nat. Rev. Mol. Cell Biol.* **2009**, *10*, 53.
[124] W. Zheng, B. Jiang, D. Wang, W. Zhang, Z. Wang, X. Jiang, *Lab Chip* **2012**, *12*, 3441.
[125] S. Chien, *Am. J. Physiol. Circ. Physiol.* **2007**, *292*, H1209.
[126] H. H. Lipowsky, S. Kovalcheck, B. W. Zweifach, *Circ. Res.* **1978**, *43*, 738.
[127] S. C. Herbert H. Lipowsky Shunichi Usami, *Microvasc. Res.* **1980**.
[128] D. Guo, S. Chien, J. Y.-J. Shyy, *Circ. Res.* **2007**, *100*, 564.
[129] F. Wang, Z. Wang, J. Pu, X. Xie, X. Gao, Y. Gu, S. Chen, J. Zhang, *Life Sci.* **2019**, *224*, 212.
[130] J. J. Chiu, D. L. Wang, S. Chein, R. Skalak, S. Usami, *J. Biomech. Eng.* **1998**.
[131] N. Wang, H. Miao, Y.-S. Li, P. Zhang, J. H. Haga, Y. Hu, A. Young, S. Yuan, P. Nguyen, C.-C. Wu, S. Chien, *Biochem. Biophys. Res. Commun.* **2006**, *341*, 1244.
[132] C. W. Ni, H. Qiu, H. Jo, *Am. J. Physiol. Circ. Physiol.* **2011**, *300*, H1762.
[133] S. C. M. Yu, *Int. J. Heat Fluid Flow* **2000**.
[134] J. Ribas, H. Sadeghi, A. Manbachi, J. Leijten, K. Brinegar, Y. S. Zhang, L. Ferreira, A. Khademhosseini, *Appl. Vitr. Toxicol.* **2016**, *2*, 82.
[135] K. Nakamori, M. Odawara, T. Nakajima, T. Mizutani, K. Tsubota, *Am. J. Ophthalmol.* **1997**, *124*, 24.
[136] U. Hampel, F. Garreis, F. Burgemeister, N. Eßel, F. Paulsen, *Ocul. Surf.* **2018**, *16*, 341.
[137] M. M. Pool, V. E. A. Post, C. T. Simmons, *Water Resour. Res.* **2015**, *51*, 1570.
[138] D. C. Miller, M. J. Bock, E. J. Turner, *J. Mar. Res.* **1992**, *50*, 489.
[139] R. Ghosh, G. A. Buxton, O. B. Usta, A. C. Balazs, A. Alexeev, *Langmuir* **2010**, *26*, 2963.
[140] J. Han, C. S. Peskin, *Proc. Natl. Acad. Sci.* **2018**, *115*, 4417.
[141] S. Uppaluri, N. Heddergott, E. Stellamanns, S. Herminghaus, A. Zöttl, H. Stark, M. Engstler, T. Pfohl, *Biophys. J.* **2012**, *103*, 1162.
[142] J. Elgeti, R. G. Winkler, G. Gompper, *Reports Prog. Phys.* **2015**, *78*, 56601.
[143] J. W. Haycock, in *3D Cell Cult.*, Springer, **2011**, pp. 1–15.
[144] M. Ni, W. H. Tong, D. Choudhury, N. A. A. Rahim, C. Iliescu, H. Yu, *Int. J. Mol. Sci.* **2009**, *10*, 5411.
[145] L. C. Espinha, D. A. Hoey, P. R. Fernandes, H. C. Rodrigues, C. R. Jacobs, *Cytoskeleton* **2014**, *71*, 435.
[146] C. R. White, J. A. Frangos, *Philos. Trans. R. Soc. B Biol. Sci.* **2007**, *362*, 1459.

[147] P. H. Krebsbach, S. A. Kuznetsov, P. Bianco, P. G. Robey, *Crit. Rev. Oral Biol. Med.* **1999**, *10*, 165.
[148] Y. J. Li, N. N. Batra, L. You, S. C. Meier, I. A. Coe, C. E. Yellowley, C. R. Jacobs, *J. Orthop. Res.* **2004**, DOI 10.101 61i.orthres.2004.04.002.
[149] D. Du, K. S. Furukawa, T. Ushida, *Biotechnol. Bioeng.* **2009**, *102*, 1670.
[150] N. L. of Enteric Pathogens, *Can. J. Infect. Dis.* **1991**, *2*, 89.
[151] P. Markoulatos, N. Siafakas, M. Moncany, *J. Clin. Lab. Anal.* **2002**, *16*, 47.
[152] C. Zhang, D. Xing, *Nucleic Acids Res.* **2007**, *35*, 4223.
[153] M. U. Kopp, *Science (80-.).* **1998**, *280*, 1046.
[154] H. Wang, C. Zhang, D. Xing, *Microchim. Acta* **2011**, *173*, 503.
[155] C. Zhang, H. Wang, D. Xing, *Biomed. Microdevices* **2011**, *13*, 885.
[156] W. Wang, Z.-X. Li, R. Luo, S.-H. Lü, A.-D. Xu, Y.-J. Yang, *J. Micromechanics Microengineering* **2005**, *15*, 1369.
[157] H.-Y. WANG, C.-S. ZHANG, Y.-Y. LI, *Chinese J. Anal. Chem.* **2009**, *37*, 1286.
[158] J. Nie, Y. Zhao, N. Peng, *Microsyst. Technol.* **2014**, *21*, 41.
[159] K. Vijayakumar, S. Gulati, A. J. deMello, J. B. Edel, *Chem. Sci.* **2010**, *1*, 447.
[160] J. P. Frampton, D. Lai, H. Sriram, S. Takayama, *Biomed. Microdevices* **2011**, *13*, 1043.
[161] C. E. Owens, A. J. Hart, *Lab Chip* **2018**, *18*, 890.
[162] Q. Ji, J. M. Zhang, Y. Liu, X. Li, P. Lv, D. Jin, H. Duan, *Sci. Rep.* **2018**, *8*, DOI 10.1038/s41598-018-22756-1.
[163] Y.-Q. Fan, H.-L. Wang, J.-J. Gao, Ke-XinLiu, D.-P. Chai, Y.-J. Zhang, *Chinese J. Anal. Chem.* **2018**, *46*, 1863.